Volume 2 number 11 November 1975 Nucleic Acids Research

Low-angle neutron scattering from chromatin subunit particles

J. F. Pardon[1*], D. L. Worcester[2], J. C. Wooley[1], K. Tatchell[3], K. E. Van Holde[3] and B. M. Richards[1]

[1] Searle Research Labs., Lane End Road, High Wycombe, Bucks., UK

Received 13 October 1975

ABSTRACT

Monomer chromatin particles containing 140 base pairs of DNA and eight histone molecules have been studied by neutron scattering. From measurements in various H_2O/D_2O mixtures, radii of gyration and the average scattering density of the particle were determined. The radius of gyration under conditions when scattering from the DNA dominates is 50Å, and when scattering from the protein dominates, 30Å. Consequently the core of the particle is largely occupied by the histones while the outer shell consists of DNA together with some of the histone.

INTRODUCTION

There is now considerable evidence that chromatin largely consists of nucleoprotein subunits (1-5). Nuclease digestion studies indicate that such subunits are repetitively spaced along the DNA at intervals averaging about 180 to 200 base pairs (4,6, 7). Nucleoprotein particles can be isolated from such digests either by density gradient sedimentation (4) or by gel filtration (8). The monomer particles appear to be compact objects of roughly 100Å diameter (9,10). There is some disagreement as to whether or not all of the DNA in the repeating unit is contained as an integral and essential part of the particle (4,6,7). A number of recent studies indicate that the stable nucleoprotein particle contains about 140 base pairs of DNA, with an average interparticle DNA strand of about 40-60 base pairs (6,7,11). These "core" particles exhibit a sedimentation coefficient of about 11 S, and recent measurements indicate a molecular weight of about 200,000 daltons, of which about 90,000 daltons is DNA,

and about 110,000 daltons is protein (12). The protein is composed almost exclusively of two copies of each of the four histones $F2a_2$, F2b, F3 and $F2a_1$.

The fine structure of these particles is virtually unknown. Models have been proposed in which the DNA is wrapped about a histone core (13,14). While such a structure seems reasonable, and gains some support from the accessibility of the DNA to DNAse I (15) and neutron diffraction from whole chromatin (29), no direct evidence has been forthcoming.

In this paper we describe low-angle neutron scattering experiments with purified monomer particles from chicken erythrocyte chromatin. Neutron scattering has the following advantage over other scattering techniques: the scattering density of the suspending medium can be varied over a wide range using H_2O/D_2O mixtures. The mean scattering densities of protein and nucleic acid are within this range, corresponding to mixtures of about 0.40 and 0.60 mole fraction D_2O respectively. Therefore, conditions can be obtained in which the scattering from each individual component dominates. This method of "contrast variation" has previously been applied with success to such structures as globular proteins, low density lipoprotein, ferritin and ribosomes (16-20).

EXPERIMENTAL

1. Preparation and purification of monomer particles

Chicken erythrocyte nuclei were isolated and digested for 10 minutes with staphylococcal nuclease, as previously described (7). The reaction was terminated by adding EDTA to 10mM, and the nuclei were lysed and the lysate then applied to a Bio-Gel A-5m column, in the manner described by Shaw *et al.* (8). The "monomer" peaks from four such preparations were pooled, concentrated to 20 ml in an Amicon concentrator, and then sedimented for 20 hours at 41,000 rpm in a SW-41 rotor. Two pellets were thus obtained; one was taken up in 10mM tris, 0.7 mM EDTA buffer (pH 7.4) made with H_2O, the other in the equivalent buffer made up in D_2O. The D_2O

was redistilled from commercial D_2O (obtained from Fluorochem Ltd. U.K.) to which was added 10mg EDTA per litre. This procedure was adopted to avoid particle aggregation induced by heavy metal phosphate impurities in commercial D_2O (21). The concentrations of the two samples were 11 mg/ml. Two more samples [at 75% (v/v) D_2O, and 25% (v/v) D_2O] were later prepared by mixing appropriate portions of the original samples.

2. Tests of homogeneity and stability of particles

The success of the experiments depends upon having homogeneous particle preparations. Furthermore, since the neutron scattering experiments are of many hours' duration (see below) it was important to know that the particles remain stable over such periods. Sedimentation velocity experiments indicated that the particles were quite homogeneous, and sedimented at approximately 11 S, as in other preparations. Sucrose gradient profiles of the preparation, made before and after the entire series of neutron scattering experiments, show no change in particle size or evidence for aggregation (Figure 1). Further evidence for the stability of such preparations is given by the fact that analytical ultracentrifuge experiments on a similar preparation showed no detectable change in either $S_{20,w}$ or the boundary shape after six days' storage at room temperature.

Finally, the DNA extracted from these particles, when electrophoresed on 3·5% polyacrylamide gels, exhibited the sharp pattern typically found for the monomer (7), with an average size of 140 base pairs. In particular, neither this experiment nor the sedimentation experiments (see Figure 1) showed indication of any appreciable amount of dimers or larger particles, nor of sub-monomer fragments.

3. Neutron scattering measurements

The neutron scattering measurements were made at the PLUTO reactor of the Atomic Energy Research Establishment, Harwell. The small-angle diffractometer described by Haywood and

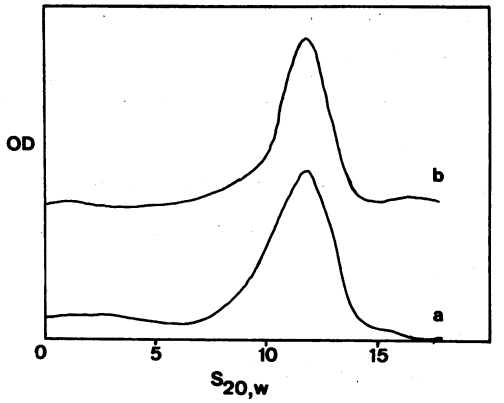

Figure 1: Sedimentation analysis of chromatin particles (a) before and (b) after the particles were used for neutron scattering measurements. Optical densities measured at 260 nm. For (b), particles were run on a 5-28% isokinetic sucrose gradient, for (a), a 2.5-26% isokinetic gradient was used.

Profile (a) was obtained before the particles were concentrated by pelleting at 41,000 rpm. This additional purification step removed the majority of material below approximately 10 S and is the reason for the narrower peak in profile (a). These profiles show that there is no change in sedimentation rate as a result of the exposure of the particles to the neutron beam for several hours at room temperature.

Worcester (22) was used to collect data over the scattering angle range $0.6 < 2\theta < 2.6^{\circ}$, incrementing 2θ in steps of 0.1°. The wavelength of neutrons was 4.67Å with a $\Delta\lambda/\lambda$ of 2%. The incident beam was collimated to 0.24° full width at half maximum using a collimator with 1 x 3 cm^2 slits inside a copper guide tube measuring 3cm x 5cm x 5m. After scattering from the sample the neutrons were analysed by a soller collimator (0.32° definition) and a graphite monochromator and detected in a BF_3 counter. All measurements were made at $23^{\circ}C$ and data was collected during scans ranging in length from four to twelve hours.

The sample volume of 0.45 ml was contained in a quartz cuvette of 2mm path length. Measurements were made with solutions containing 0, 25, 75 and 100% D_2O at a particle concentration of 11 mg/ml. Additional measurements at concentrations of 5 mg/ml and 2.5 mg/ml were made in D_2O solutions. Duplicate

runs were made for each buffer. Slit height corrections were made with a desmearing program described by Vonk (23) as used by D. Sadler at the University of Bristol.

Radii of gyration and uncertainties were calculated from least squares linear fits of log (intensity) vs. h^2 where $h = 4\pi \sin\theta/\lambda$. The Guinier plots were linear for the range of scattering angle (2θ) scanned, as determined by evaluation of χ^2 for the linear fits.

RESULTS AND DISCUSSION

Typical Guinier plots of the neutron scattering data are shown in Figure 2. From the least squares linear fits to these data, the zero angle scattering intensity was obtained, corrected for absorption and plotted as a function of the D_2O molar percen-

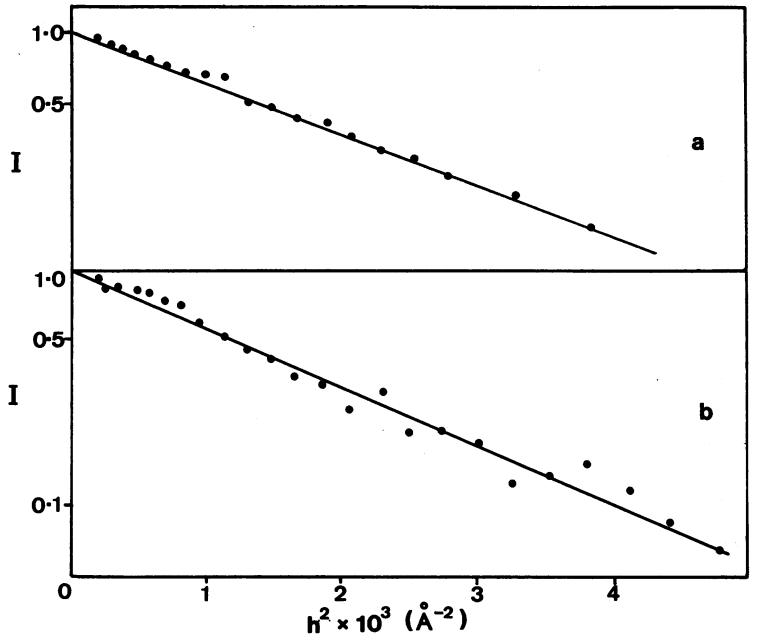

Figure 2: Examples of Guinier plots obtained from chromatin particles (a) Particles in D_2O (b) in H_2O. Semi-log plot of intensity (I) versus h^2, where $h = 4\pi \sin\theta/\lambda$ and 2θ is the angle of scattering. Each data set is fitted with a straight line by a variance-weighted least squares procedure. The data are arbitrarily scaled with respect to I for convenience in plotting them on the same graph.

tage of the buffer. A graph of $I_o^{\frac{1}{2}}$ vs. D_2O mole fraction (Figure 3) is linear and the zero intensity intercept gives the D_2O concentration at which the mean scattering density of the chromatin particle (ρ_c) equals that of the solvent (ρ_s). The experimental value of 49% D_2O is also the value predicted from the composition of the particles (1.25 mg protein/gm DNA) and the mean scattering length densities of the components with 76% of the labile protons exchanging with the solvent (25,26).

The slope of the Guinier plot allows calculation of the radius of gyration (24), from the equation:

$$\text{Slope} = {}^1/_3 R^2 \qquad (1)$$

The experimental values for the radii of gyration, obtained both before and after corrections for slit smearing, are shown in Table 1. No significant concentration dependence was found in the range 2.5 - 11 mg/ml.

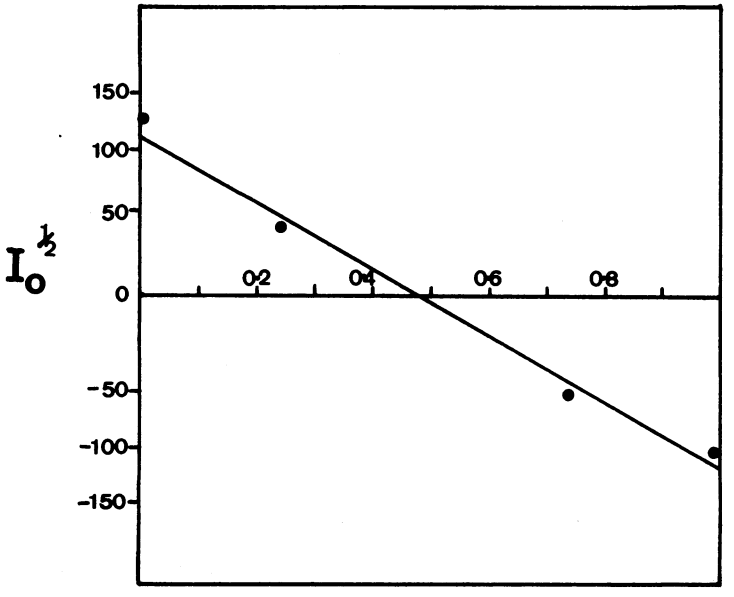

Figure 3: Plot of square root of zero angle scattering intensity ($I_o^{\frac{1}{2}}$) versus mole fraction of D_2O in the buffer. The least squares intercept for $I_o^{\frac{1}{2}} = 0$ is at 0.49.

TABLE 1

Percentage D_2O in Buffer	Particle Concentration mg/ml	Radius of Gyration (not corrected) Å	Radius of Gyration (corrected for slit smearing) Å
100	11	38.4 ± 0.3	39.1 ± 0.3
100	5	38.2 ± 0.3	
100	2.5	35.9 ± 1.1	
75	11	36.3 ± 0.9	36.8 ± 0.9
25	11	45.3 ± 6.0	49.9 ± 5.5
0	11	41.8 ± 0.7	43.0 ± 0.7

The radius of gyration of an object with internal variation of scattering density, as measured by neutron scattering, is a function of the scattering density and hence the isotopic composition of the suspending medium. Stuhrmann (16) has demonstrated that for an inhomogeneous but centrosymmetric body, the radius of gyration, R, will vary as:

$$R^2 = R_I^2 + \frac{\alpha}{\bar{\rho}} \qquad (2)$$

Here, $\bar{\rho} = \rho_c - \rho_s$, is the difference between the mean scattering density of the chromatin particle and that of the buffer and R_I is the radius of gyration for infinite contrast between particle and buffer. R_I is also the radius of gyration for a particle of the same shape and dimensions, but homogeneous, with no internal variation of scattering density. If the regions of different scattering density in the particle do not have the same centre of mass, equation (2) no longer applies. A graph of R^2 vs. $1/\bar{\rho}$ will then be curved, rather than linear (18).

$$R^2 = R_I^2 + \frac{\alpha}{\bar{\rho}} + \beta/\bar{\rho}^2 \qquad (3)$$

Figure 4 depicts our data graphed according to equation (3). While the present data are not sufficiently accurate to preclude some small curvature, the simplest fit is a straight line. The pronounced slope of the line shows that the particles are composed of regions of very different scattering density. The value of α obtained for the chromatin particles is 508 (± 80) x 10^{-6} which is smaller than found for lipoprotein, 2800 x 10^{-6} (18),

and more than a factor of ten larger than found for a number of globular proteins (16), e.g. $\alpha = 35 \times 10^{-6}$ for myoglobin (17) and lysozyme (27). Furthermore, the sign of the slope demonstrates that the radius of gyration for the material with higher scattering density (the DNA) is greater than that for the material of lower scattering density (the protein). Thus, this result demonstrates that the mass of DNA is concentrated towards the outside of the particle.

By extrapolating the graph to those points at which the scattering density of the buffer is the same as the mean scattering density of either DNA or protein, one obtains R^2 for the conditions in which either the DNA or the protein dominates the scattering and hence the value of the radius of gyration.

The mean scattering densities of the DNA and the histones can be calculated from the coherent scattering amplitudes (28) and the partial specific volumes of these components (25,26) provided the extent of H/D exchange with the solvent is known.

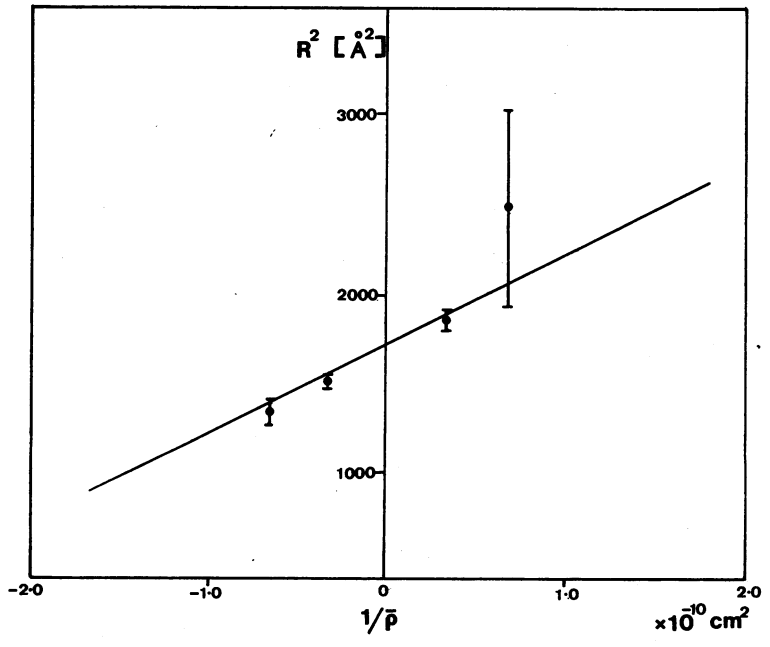

Figure 4: The variation in R^2 as a function of $1/\bar{\rho}$

We estimate from the zero intensity intercept of the zero-angle scatter (49% D_2O), that 76% of the labile protons of the chromatin particles are exchanging with the solvent. The exchange for the individual components however is unknown, so we have assumed complete exchange for the DNA. This seemed a reasonable assumption because we have established that the DNA is concentrated toward the outside of the particle; it is also readily hydrated. Under this condition the mean scattering densities of the DNA and the water are equal for 60.5% D_2O. With the assumption of complete exchange for the DNA, only 68% of the labile protons of the histones are exchanging with the solvent. Under this condition, the mean scattering densities of the protein and the water are equal for 39.0% D_2O.

Using the values of $\bar{\rho}$ for 60.5% and 39% D_2O solvent we have evaluated the radius of gyration when the protein dominates (R_P) and when the DNA dominates (R_D) respectively, using equation (3) and the fitted values for R_I^2 and α with $\beta = 0$. These results are summarised in Table II.

TABLE II

	$1/\bar{\rho}$ (cm^2)	R (Å)
$R = R_P$ (Protein dominates)	-1.49×10^{-10}	30.6 (± 2.0)
$R = R_D$ (DNA dominates)	1.69×10^{-10}	50.5 (± 1.4)
$R = R_I$ (Infinite contrast)	0	41.1 (± 0.4)

Since the above value of R_I as well as electron microscope and hydrodynamic studies (12) indicate a particle radius of about 50Å, the value obtained for R_D (50.5Å) immediately demonstrates that the DNA is on, or very near, the particle surface. These values of R_D and R_P are not critically dependent on the exact nature of the H-D exchange, but should not yet be taken as precise radii of gyration for the DNA and protein components since it has not yet been established that scattering density variations within the DNA and protein do not contribute when the mean scattering densities are equal to the solvent. Scattering density variations

from a hydrophobic interior to a polar exterior are a common feature of many globular proteins (16) and may occur in the chromatin particle. However, we have calculated that the scattering density differences between the more hydrophobic C-terminal portions and the more polar N-terminal portions of the histones are small. For example, there is no difference for histone F2B, and a maximum of 2.6 x 10^{-15} cm/Å^3 difference for histone $F2A_1$. Therefore, differences in H-D exchange are the only probable source of spatial variations in the protein scattering density.

We also emphasise that data at lower contrasts is needed to better establish whether or not $\beta = 0$. However, because β is required to be negative (17), any non-zero value for β will lower R_D and R_p.

Interpretations Based on Models

The data can be further interpreted if specific centrosymmetric models are considered. It must be emphasised that such models are probably oversimplifications, for neither the protein, nor the DNA, are necessarily distributed uniformly over regions of simple shape. Two simple models are presented to demonstrate the kinds of structure that are able to account for the three radii of gyration R_p, R_D and R_I.

Model A (figure 5A) is a spherical particle with a sphere of density ρ_p surrounded by a shell of density ρ_D. It resembles the "bead" structure proposed by Kornberg (13) in which the eight histones form a globular core with DNA arranged on the outside. Model B (figure 5B) has a cylindrical core of density ρ_p surrounded by a DNA helix. In some respects model B resembles the model suggested by Langmore and Wooley (9).

The sphere shown in model A has an overall diameter derived from R_I of 106Å; the material of high scattering density (DNA) is depicted as being distributed within an outer shell of 20Å thickness. The radius of gyration of the DNA (50.5 $\pm$ 1.4Å) falls within the shell. There is some overlap between the protein and the DNA in the region radius 33Å to 41Å, the latter being derived

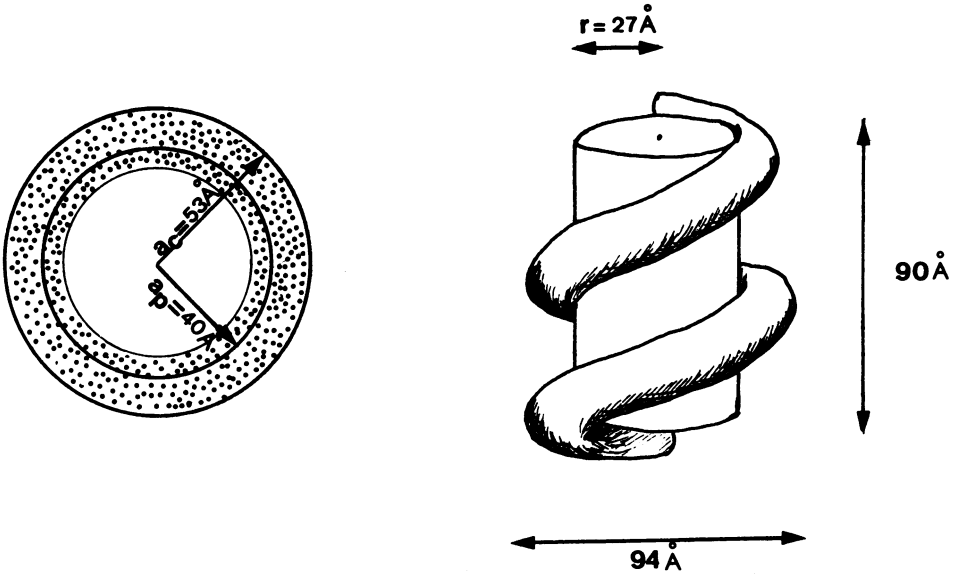

Figure 5: Two possible kinds of structure for the chromatin particle containing 140 base pairs of DNA and eight histones. (a) A spherical particle with overall diameter a_c = 53Å, derived from R_I = 41.1, in which the inner protein core has radius a_p = 40 from the experimental R_p = 30.6Å. The region occupying the DNA is shaded.
(b) A cylindrical model in which two turns of helix with pitch 45Å and radius 37Å wound on an inner protein core of radius 27Å.

from the expression relating radius of gyration (R) to overall radius (a) for a sphere of uniform scattering density, i.e. $a^2 = {}^5/_3 R^2$. For R_p = 30.6, a is 40Å. The anhydrous volume for the eight histone molecules is a sphere of radius 32Å. Clearly the total volume of this model exceeds the partial specific volume for a particle consisting of eight histones and 140 base pairs of DNA. This difference could result from a combination of internal hydration and the existence of either a central hole (9) or depressions on the surface. Model A predicts a Stokes' Law effective diameter of 106Å, in good agreement with the value of 107Å obtained from the sedimentation velocity and the M $(1 - \bar{v}\rho)$ obtained from sedimentation equilibrium studies (7).

For model B, the DNA is wound on a cylindrical protein core.

Calculations show that a series of pairs of values for the radius and height of the core can be used to account for the experimental R_p = 30.6Å. The model shown is one such example with a core radius of 27Å and height 90Å. The DNA has to be included in such a configuration that the 140 base pairs have an approximate radius of gyration of 50Å. In the model two turns of DNA are wound around the protein core in a helix of radius 37Å and pitch 45Å. It was not possible to derive a cylindrical model with less than 1½ turns of DNA around an inner protein core.

Both of these models, developed from the low angle neutron scattering data, are consistent with what we know about the particles. At this stage in the collection of data further speculation concerning the arrangement of DNA and histones within the particle is not useful. It is now necessary to extend the scattering data to smaller values for the contrast and to higher scattering angles in order to limit the choice of possible models.

Acknowledgements

We wish to acknowledge the expert assistance of Ms. Leslei Lewis and Mrs. Hazel Briggs with sedimentation experiments. One of us (KVH) was aided by an EMBO Fellowship; another (JCW) was supported by a Searle Visiting Fellowship. The work was supported in part by NSF Grant BMS 73-06819 A02. We are indebted to Dr. D. Sadler for assisting us in using his version of the Vonk desmearing program.

Finally we thank both Dr. A.J. Hale and Dr. B.T.M. Willis for their generous support in providing both encouragement and facilities.

2. Material Physics Division, AERE Harwell.

3. Department of Biochemistry and Biophysics, Oregon State University, Corvallis, OR 97331, USA

*To whom requests for reprints should be addressed

REFERENCES

1. Hewish, D.R. and Burgoyne, L.A. (1973) Biochem. Biophys. Res. Comm. 52, 504-510
2. Sahasrabuddhe, C.G. and Van Holde, K.E. (1974) J. Biol. Chem. 249,152-156
3. Olins, D.E. and Olins, A.L. (1974) Science 184, 330-332
4. Noll, M. (1974) Nature 251, 249-251
5. Oudet, P., Gross-Bellard, M. and Chambon, P. (1975) Cell 4, 281-300
6. Sollner-Webb, B. and Felsenfeld, G. (1975) Biochemistry 14, 2915-2920
7. Shaw, B.R., Herman, T.M., Kovacic, R.T., Beaudreau, G.S. and Van Holde, K.E. (1975) Proc. Natl. Acad. Sci. USA. In Press.
8. Shaw, B.R., Corden, J.L., Sahasrabuddhe, C.G. and Van Holde, K.E. (1974) Biochem Biophys. Res. Comm. 61, 1193-1198
9. Langmore, J.P. and Wooley, J.C. (1975) Proc. Natl. Acad. Sci. USA 72, 2691-2695
10. Van Holde, K.E., Sahasrabuddhe, C.G., Shaw, B.R., Van Bruggen, E.F.J. and Arnberg, A. (1974) Biochem. Biophys. Res. Comm. 60, 1365-1370
11. Axel, R. (1975) Biochemistry 14, 2921-2925
12. Van Holde, K.E., Shaw, B.R., Lohr, D., Herman, T.M. and Kovacic, R.T. (1975) Proc. 10th FEBS Meetings, Paris. In Press.
13. Kornberg, R.D. (1974) Science 184, 868-871
14. Van Holde, K.E., Sahasrabuddhe, C.G. and Shaw, B.R. (1974) Nucleic Acids Res. 1, 1579-1586
15. Noll, M. (1974) Nucleic Acids Res. 1, 1573-1578
16. Stuhrmann, H.B. (1974) J. App. Cryst. 7, 173-178
17. Ibel, K. and Stuhrmann, H.B. (1975) J. Mol. Biol. 93, 255-265
18. Stuhrmann, H.B., Tardieu, A., Mateu, L., Sardet, C., Luzzati, V., Aggerbeck, L. and Scanu, A.M. Proc. Nat. Acad. Sci. USA 72, 2270-2273
19. Moore, P.B., Engelman, D.M. and Schoenborn, B.P. (1974) Proc. Nat. Acad. Sci. USA 71, 172-176
20. Moore, P.B., Engelman, D.M. and Schoenborn, B.P. (1975) J. Mol. Biol. 91, 101-120
21. Huxtable, R., and Bresster, R. (1974) J. Memb. Biol. 17, 189-197
22. Haywood, B.C.G. and Worcester, D.L. (1973) J. Phys. E. 6, 586-571
23. Vonk, C.G. (1974) J. Appl. Cryst. 4, 340-342
24. Guinier, A. and Fournet, G. (1955) Small Angle Scattering of X-rays, Wiley and Sons, New York.
25. Zamyatnin, A.A. (1972) Prog. Biophys. and Mol. Biol. 241, 109-123
26. Langridge, R., Marvin, D.A., Seeds, W.E., Wilson, H.R., Hooper, C.W., Wilkins, M.H.F. and Hamilton, L.D. (1960) J. Mol. Biol. 2, 38-64

27. Stuhrmann, H.B. and Fuess, H. (1974) Report no. 74S158 of the Institute Laue Langevin, Grenoble and Acta. Cryst. A. (In Press, 1975)
28. Bacon, G.E. (1962) Neutron Diffraction. Oxford University Press.
29. Baldwin, J.P., Boseley, P.G. and Bradbury, E.M. (1975) Nature 253, 245-249.